Polyhedron 228 (2022) 116176

Contents lists available at ScienceDirect

Polyhedron

journal homepage: www.elsevier.com/locate/poly

# Complex structures, formation thermodynamics and substitution reaction kinetics in the copper(II) – glycylglycyl-L-tyrosine – L/D-histidine systems

Nikita Yu. Serov [a], Valery G. Shtyrlin [a,*], Mikhail S. Bukharov [a], Anton V. Ermolaev [a], Edward M. Gilyazetdinov [a], Kira V. Urazaeva [a], Alexander A. Rodionov [b]

[a] A.M. Butlerov Chemistry Institute, Kazan University, Kremlevskaya st. 18, 420008 Kazan, Russian Federation
[b] Institute of Physics, Kazan University, Kremlevskaya st. 18, 420008 Kazan, Russian Federation

ARTICLE INFO

*Keywords:*
Complex formation
Substitution kinetics
Stereoselective effects
Glycylglycyl-L-tyrosine
Histidine
Copper(II)

ABSTRACT

Complex formation thermodynamics in the copper(II) – glycylglycyl-L-tyrosine (GGY•H) and copper(II) – glycylglycyl-L-tyrosine – L/D-histidine (HisH) systems (25.0 °C, 1.0 M $KNO_3$) was investigated by pH-potentiometric titration and spectrophotometry methods in a wide pH range (2–11). As a result five homoligand and six heteroligand complexes were discovered for the first time. Parameters of individual absorption spectra and ESR spectra of the heteroligand copper(II) complexes were first evaluated. Structures of complexes were optimized by DFT computations on the B3LYP/TZVPP level with accounting solvent effect by the C-PCM model and with dispersion correction (D3BJ). Based on the experimental data and the results of quantum chemical computations, it was suggested that there is a *d*-π interaction between the aromatic system of tyrosine and copper(II) in homoligand complexes with a metal/ligand ratio of 1:1. The stereoselective effect in the formation of Cu(GGY)(His) form having higher stability of complex with L-histidine relative to D-histidine was revealed and explained in terms of trans-influence and π-π-stacking interactions, that was confirmed by quantum-chemical calculations. Using stopped-flow technique with spectrophotometric detection, the kinetics of glycylglycyl-L-tyrosine substitution by L/D-histidine was investigated and three-step scheme of the ligand replacement was proposed. The stereoselective effect in substitution of the glycylglycyl-L-tyrosine by histidine with faster process for D-$His^-$ than to L-$His^-$ form was detected and explained on the basis of the formation of heteroligand intermediates.

## 1. Introduction

The largest task of modern science is to understand the specificity and selectivity of processes in living nature, which is directly related to solving the fundamental problem of the origin of life. To solve this task, a deep study of the regularities of metal–ligand, weak inter-ligand, outer-sphere interactions and solvation in complex formation processes that underlie the functioning of biological systems, is required. Probably already at the first stages of biochemical evolution, an important role was played by the selectivity of coordination processes of amino acids, oligopeptides, nucleotides, oligonucleotides and sugars to metals. Unfortunately, the factors controlling the specificity and selectivity of the complex formation processes of biometals with bioligands are still insufficiently studied. In order to identify these factors, we previously studied in detail the effects of stereoselectivity manifested in the structure, formation thermodynamics and kinetics of the ligands substitution reactions of homo- and heteroligand complexes in the aqueous solutions of copper(II) and nickel(II) with enantiomerically homogeneous and racemic forms of histidine and methionine [1,2]. Complexes containing histidine deserve great attention, since they are involved in the biological transport of metals [3], and in addition, the histidine residue is incorporated into many metallo-enzymes [4].

Copper(II) complexes with oligopeptides are of special interest for inorganic biochemistry as mediators, models of metal enzymes, and transport forms in living organisms. In our previous work [5] we investigated the complex formation thermodynamics, spectral parameters, complex structures and substitution reaction kinetics in the copper(II) – glycylglycylglycine – L/D/DL-histidine systems at 25.0 °C with 1.0 M $KNO_3$ background. Current work is a continuation of the previous study and is devoted to homo- and heteroligand complexes of copper(II) with glycylglycyl-L-tyrosine and histidine.

It should be mentioned that there are only several works [6–8] dealing with copper(II) complexes including tyrosine-containing tripeptides. In the works [7,8] it was found that glycylglycyl-L-tyrosine,

* Corresponding author.
*E-mail address:* Valery.Shtyrlin@gmail.com (V.G. Shtyrlin).

https://doi.org/10.1016/j.poly.2022.116176
Received 15 August 2022; Accepted 14 October 2022
Available online 22 October 2022

glycyl-L-leucyl-L-tyrosine, glycyl-L-tyrosylglycine and L-tyrosylglycylglycine give the same complex forms: $CuLH^{+}$, CuL, $CuLH_{-1}^{-}$ and $CuLH_{-2}^{2-}$. In the earlier work [6] copper(II) complexes with glycyl-L-leucyl-L-tyrosine and L-tyrosylglycylglycine were investigated by the absorption spectroscopy, NMR and EPR methods. On the basis of spectral data the interaction between aromatic ring and metal ion was established. Weak interaction between copper(II) and phenoxyl fragment of glycyl-L-leucyl-L-tyrosine was proposed earlier based on the X-ray analysis data of complex crystals grown at neutral pH [9].

Several investigations [10,11] are devoted to complex formation between copper(II) and glycylglycyl-L-tyrosine-*N*-methyl amide – a peptide mimicking the $NH_2$-terminal copper(II) binding site of dog serum albumin. It was concluded that the absence of any charge transfer band around 400 nm strongly indicates that Cu(II) does not bind to the phenoxyl group [10]. It was also said that NMR results are consistent with the noninvolvement of the tyrosine residue of glycylglycyl-L-tyrosine-*N*-methyl amide in copper(II) complexation. Such conclusion is contradictory with revealed weak interaction between tripeptide tyrosine residue and copper(II) in solution [6] and in solid phase [9].

There is no any information about the ternary complexes of copper (II) with tyrosine-containing tripeptides and amino acids in the literature. We especially note that the fundamental problem of stereoselectivity in complex formation and ligand substitution reactions with participation of oligopeptides requires further deep development.

## 2. Experimental

### 2.1. Materials

Copper(II) nitrate of analytical grade, D-histidine (Sigma), L-histidine (Reanal), and glycylglycyl-L-tyrosine (Bachem) were used in this work. The NaOH (Sigma) and HCl solutions of analytical grade have been employed at pH-potentiometric titration. The KOH (Chemapol) and $HNO_3$ solutions of analytical grade were also used to maintain the acidity of the medium. Adding $KNO_3$ of analytical grade (AppliChem) recrystallized from aqueous solution was provided to salt background of 1.0 M. Trilonometric titration was used to examine the concentration of the copper(II) stock solution. The titrant NaOH (with 1.0 M $KNO_3$) and titratable freshly prepared solutions were continuously blown with argon in the process of the pH-potentiometric experiment. Trizma base (Sigma) with 0.1 M concentration was used as a buffer in the kinetic experiments.

### 2.2. Methods

The automatic titrator 907 Titrando (Metrohm) with the Metrohm 6.0258.010 glass electrode was used for determination of the pH values and titrations. Measurement error of the pH value was checked and averaged ±0.001 pH unit. Standard buffer solutions were used for electrode calibration. The tangent of the slope of the calibration dependencies was within 1.000±0.001. Full agreement of the pH values of the standard buffer before and after titration testified to the reproducibility of the results. Each titration was reproduced twice.

Perkin-Elmer Lambda EZ-210 spectrophotometer was used for registration of electronic absorption spectra in 0.2 and 1.0 cm quartz cells. Optical densities of the copper(II) containing solutions were determined relatively to the solutions with background electrolyte without copper(II). Accuracy of optical density measurements was ±0.001 log. units.

The STALABS computer program [2,12] have been used for all calculations of the equilibrium constants and electron absorption spectra. The Hamilton's *R*-factor values of no more than 0.0015 for the metal–ligand system pH-potentiometric titrations and 0.05 for the spectrophotometric data have been assumed as a main criterion of adequacy of the experimental data description.

To obtain X-band ESR spectra at room temperature (r.t.), Bruker ESP 300 spectrometer was used. For record the ESR spectra two thin tubes (1 mm outer diameter) with sample were placed inside a single 5 mm diameter tube. The ESR spectra have been simulated with the EasySpin software package [13]. The rotational correlation times $\tau_R$, isotropic $g_0$ factors, hyperfine coupling constants $A_0$, and superhyperfine coupling constants $A_N$ were obtained by the simulations.

The spectrophotometer Cary 50 Bio (Varian) with the Rapid Mix RX2000 (Applied Photophysics) spectrophotometric accessory were utilized for the ligand substitution reactions kinetics investigation by the stopped-flow method in the pseudo first-order conditions by the concentration of histidine. For the one set of experimental conditions, the kinetic dependencies were reproduced at least 5 times. Circulating thermostat Julabo F25-HL for the temperature control in solutions with an accuracy of ±0.05 °C has been used at the pH-metric titrations and kinetic experiments.

Structures of complexes have been optimized with the ORCA program [14] using the DFT method [15] at the B3LYP/TZVPP level [16–20] with the accounting solvent effect by the C-PCM model [21]. Atom-pairwise dispersion correction with the Becke-Johnson damping scheme (D3BJ) [22,23] was used to take into account possible interactions involving the aromatic fragment of the tripeptide side chain. All optimized structures were checked for the absence of the imaginary frequencies.

## 3. Results and discussion

### 3.1. Composition, stability and structure of complexes in the copper(II) – glycylglycyl-L-tyrosine system

Initially protonation constants of glycylglycyl-L-tyrosine were determined by pH potentiometric titration. Found values ($pK_{a1}$ = 3.244 (1), $pK_{a2}$ = 8.012(3) and $pK_{a3}$ = 9.860(4), in parentheses standard deviations σ are given) are in relatively good agreement with literature data [8] ($pK_{a1}$ = 3.20(1), $pK_{a2}$ = 7.91(1) and $pK_{a3}$ = 9.75(1), 25.0 °C, 0.2 M $KNO_3$). Differences between the literature data and our results may be explained by the different concentrations of the salt background.

Further the copper(II) – glycylglycyl-L-tyrosine system at different metal/ligand ratios was investigated. For 1:1 and 1:2 metal/ligand ratios the titration curves (as the Bjerrum function dependencies on pH) are given in Fig. 1S (ESI) as an example. For the found copper(II) complexes with glycylglycyl-L-tyrosine the compositions and formation constants were determined and are given in Table 1. It should be noted that nine complex forms were described in the investigated system including three *bis*-complexes and one binuclear coordination compound. Only four complex forms of copper(II) with glycylglycyl-L-tyrosine are known in literature (see Table 1). Another five complex forms, including *bis*-complexes $Cu(GGY)_2$, $Cu(GGY)(GGY{\bullet}H_{-1})^{-}$ and $Cu(GGY{\bullet}H_{-1})_2^{2-}$, binuclear form $Cu_2(GGY{\bullet}H_{-1})_2$ and $Cu(GGY{\bullet}H)^{2+}$, were determined for the first time.

As can be seen from the Table 1 the data, obtained in this work, and the literature data [8] for the complex formation between copper(II) and

**Table 1**
Formation constant logarithms (log β) of complexes in the copper(II) – glycylglycyl-L-tyrosine system (25.0 °C, 1.0 M $KNO_3$) in comparison with literature data [8] (25.0 °C, 0.2 M $KNO_3$).

| N | Equilibrium | log β | log β [8] |
|---|---|---|---|
| 1 | $Cu^{2+} + GGY{\bullet}H \rightleftharpoons Cu(GGY{\bullet}H)^{2+}$ | 1.920(2) | – |
| 2 | $Cu^{2+} + GGY^{-} \rightleftharpoons Cu(GGY)^{+}$ | 5.296(1) | 4.88(33) |
| 3 | $Cu^{2+} + GGY^{-} \rightleftharpoons Cu(GGY{\bullet}H_{-1}) + H^{+}$ | −0.230(1) | 0.07(6) |
| 4 | $Cu^{2+} + GGY^{-} \rightleftharpoons Cu(GGY{\bullet}H_{-2})^{-} + 2H^{+}$ | −6.630(2) | −6.80(8) |
| 5 | $Cu^{2+} + GGY{\cdot}H_{-1}^{2-} \rightleftharpoons Cu(GGY{\bullet}H_{-3})^{2-} + 2H^{+}$ | −6.547(3) | −7.50(13) |
| 6 | $Cu^{2+} + 2GGY^{-} \rightleftharpoons Cu(GGY)_2$ | 8.76(3) | – |
| 7 | $Cu^{2+} + 2GGY^{-} \rightleftharpoons Cu(GGY)(GGY{\bullet}H_{-1})^{-} + H^{+}$ | 3.512(5) | – |
| 8 | $Cu^{2+} + 2GGY^{-} \rightleftharpoons Cu(GGY{\bullet}H_{-1})_2^{2-} + 2H^{+}$ | −4.70(5) | – |
| 9 | $2Cu^{2+} + 2GGY^{-} \rightleftharpoons Cu_2(GGY{\bullet}H_{-1})_2 + 2H^{+}$ | 1.44(1) | – |

glycylglycyl-L-tyrosine are not in good agreement. The reasons of such situation can be the different salt backgrounds, the absence of some complex forms in literature data and smaller pH range (only up to 10 pH value) used in the work [8]. It should be mentioned that without five new complex forms the description of the experimental data (pH potentiometric data at 1:2 metal/ligand ratio, spectrophotometry and EPR data) is not satisfactory.

Fig. 1 and Fig. 2S show calculated distribution diagrams for the copper(II) – glycylglycyl-L-tyrosine system at 1:1 and 1:2 metal/ligand ratios respectively. It can be seen from the figures that in slightly alkaline conditions (pH 7–9) the form with two deprotonated peptide atoms ($Cu(GGY{\bullet}H_{-2})^{-}$) predominates. In more alkaline medium deprotonation of tyrosine fragment takes place and $Cu(GGY{\bullet}H_{-3})^{2-}$ complex is formed.

The spectrophotometric titration was also performed. The obtained individual absorption spectra of homoligand copper(II) complexes with glycylglycyl-L-tyrosine were further used for ternary system investigation. Electronic absorption spectra of the solutions at different pH and the dependencies of extinction coefficient at different wavelengths on pH are shown in Figs. 3S and 4S at 1:1 metal/ligand ratio. The distribution diagram for experimental conditions is given in Fig. 5S. To obtain the individual absorption spectra of the *bis*-complexes several spectra of the system at the 1:2 metal/ligand ratio were recorded. Reconstructed spectra are given in Fig. 2 and the total spectral parameters are presented in Table 1S.

According to the EPR data (Table 2, Fig. 6S) in the equatorial plane of $Cu(GGY{\bullet}H_{-2})^{-}$ and $Cu(GGY{\bullet}H_{-3})^{2-}$ complexes the amino group, two deprotonated peptide nitrogens and carboxy-group are coordinated (Fig. 3). Thus the equatorial coordination of glycylglycyl-L-tyrosine in these complexes is very close to the coordination of glycylglycylglycine in the $Cu(GGG{\bullet}H_{-2})^{-}$ form (see superhyperfine coupling constants $A_N$ in Table 2 and in the work [5]). However, for the considered complexes with glycylglycyl-L-tyrosine the $g_0$ factors are smaller and hyperfine coupling constants $A_0$ are bigger than for the complex with glycylglycylglycine, which can be explained by the presence of *d*-π-interaction between copper(II) and aromatic fragment of tyrosine residue. The result of such interaction is axial coordination of glycylglycyl-L-tyrosine side chain which is confirmed by quantum-chemical calculations results (Fig. 3).

The phenoxyl group deprotonation of glycylglycyl-L-tyrosine has practically no effect on tripeptide coordination that can be concluded from the similarity of the $Cu(GGY{\bullet}H_{-2})^{-}$ and $Cu(GGY{\bullet}H_{-3})^{2-}$

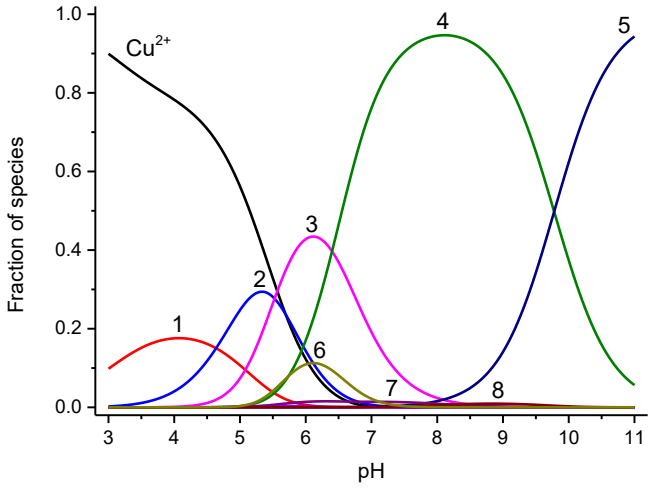


**Fig. 1.** Species distribution as a function of pH for the copper(II) – glycylglycyl-L-tyrosine system with the 1:1 metal/ligand ratio at 25.0 °C; $c_{Cu(II)} = 3.801{\cdot}10^{-3}$ M, $c_{GGY{\cdot}H} = 3.999{\cdot}10^{-3}$ M, 1.0 M $KNO_3$; 1 – $Cu(GGY{\bullet}H)^{2+}$, 2 – $Cu(GGY)^{+}$, 3 – $Cu(GGY{\bullet}H_{-1})$, 4 – $Cu(GGY{\bullet}H_{-2})^{-}$, 5 – $Cu(GGY{\bullet}H_{-3})^{2-}$, 6 – $Cu_2(GGY{\bullet}H_{-1})_2$, 7 – $Cu(GGY)(GGY{\bullet}H_{-1})^{-}$, 8 – $Cu(GGY{\bullet}H_{-1})_2^{2-}$.

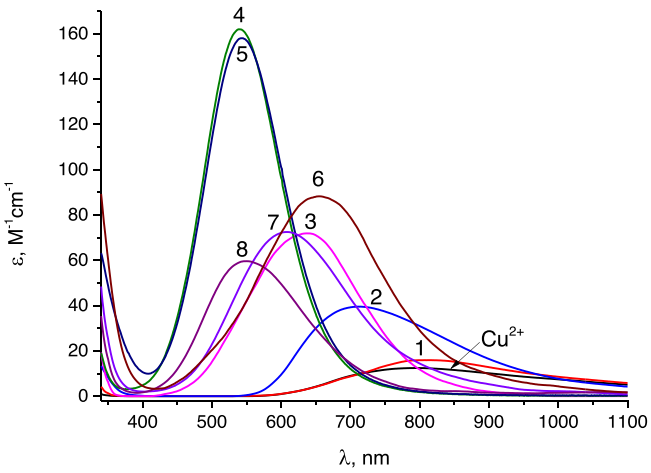


**Fig. 2.** Reconstructed electronic absorption spectra of the complexes in the copper(II) – glycylglycyl-L-tyrosine system at 25.0 °C on the 1.0 M $KNO_3$ background: 1 – $Cu(GGY{\bullet}H)^{2+}$, 2 – $Cu(GGY)^{+}$, 3 – $Cu(GGY{\bullet}H_{-1})$, 4 – $Cu(GGY{\bullet}H_{-2})^{-}$, 5 – $Cu(GGY{\bullet}H_{-3})^{2-}$, 6 – $Cu_2(GGY{\bullet}H_{-1})_2$, 7 – $Cu(GGY)(GGY{\bullet}H_{-1})^{-}$, 8 – $Cu(GGY{\bullet}H_{-1})_2^{2-}$.

**Table 2**
ESR spectra parameters of the homo-ligand copper(II) complexes with glycylglycyl-L-tyrosine (r.t., 1.0 M $KNO_3$).

| N | Complex | $g_0$ | $A_0$, G | $A_N$, G |
|---|---|---|---|---|
| 1 | $Cu(GGY{\cdot}H)^{2+}$ | 2.186(1) | 37(1) | – |
| 2 | $Cu(GGY)^{+}$ | 2.161(1) | 44(1) | 9.0(5) |
| 3 | $Cu(GGY{\cdot}H_{-1})$ | 2.1248(2) | 59.4(4) | 13.2(5), 11.8(5) |
| 4 | $Cu(GGY{\bullet}H_{-2})^{-}$ | 2.0918(2) | 83.6(2) | 17.5(2), 14.6(2), 8.2(3) |
| 5 | $Cu(GGY{\bullet}H_{-3})^{2-}$ | 2.0925(2) | 83.0(2) | 17.2(2), 14.7(2), 8.3(3) |
| 6 | $Cu_2(GGY{\bullet}H_{-1})_2$ | 2.108(2) | – | – |

complexes absorption spectra (Fig. 2), ESR spectra parameters (Table 2) and quantum-chemical calculations results (Fig. 3).

The $Cu(GGY{\bullet}H)^{2+}$ and $Cu(GGY{\bullet}H_{-1})$ complexes have also bigger formation constants than the similar forms with glycylglycylglycine (see work [5]) that can be explained by the presence of *d*-π-interaction between copper(II) and aromatic fragment of tyrosine residue. Quantum-chemical calculations results (Fig. 7S) show that the isomers of the mentioned complexes with such interaction have lower energies than the isomers without such interaction. It should be mentioned that in the complex isomers with *d*-π-interaction the distance between copper(II) and the closest carbon atom of the phenoxyl ring is in relatively good agreement with similar distance in the crystal of copper(II) with glycyl-L-leucyl-L-tyrosine [9].

### 3.2. *Composition and stability of complexes in the copper(II) – glycylglycyl-L-tyrosine – L/D-histidine system*

Potentiometric titration curves (as the Bjerrum function dependencies on pH) for the copper(II) – glycylglycyl-L-tyrosine – L/D-histidine system at 1:1:1 metal/ligand/ligand' ratio are given in Fig. 8S. Fig. 9S shows the example of calculated species distribution for heteroligand system with L-histidine. The determined compositions and formation constants of the found heteroligand complexes are given in Table 3.

The data on the copper(II) – histidine system and protonation constants of histidine necessary for modeling ternary system with glycylglycyl-L-tyrosine and histidine were taken from the work [1].

As can be seen from Table 3, six heteroligand complexes were described in the copper(II) – glycylglycyl-L-tyrosine – L/D-histidine system, including two binuclear forms with one tripeptide and two histidine molecules. Statistically meaningful stereoselectivity (when

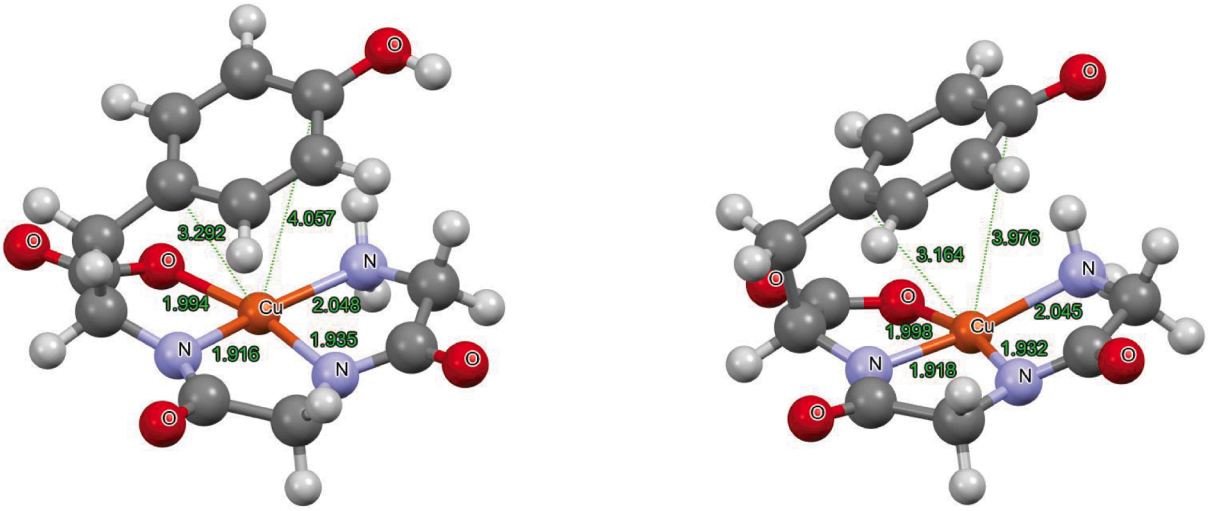


$Cu(GGY{\cdot}H_{-2})^{-}$
$E = -2684.86626$ a.u.

$Cu(GGY{\cdot}H_{-3})^{2-}$
$E = -2684.37763$ a.u.

**Fig. 3.** Structures and formation energies (in atomic units, a.u.) of the copper(II) complexes with glycylglycyl-L-tyrosine optimized on the B3LYP/TZVPP level with accounting solvent effects in the C-PCM model and dispersion correction (D3BJ).

**Table 3**
Formation constant logarithms (log β) of heteroligand complexes in the copper (II) – glycylglycyl-L-tyrosine – L/D-histidine system (25.0 °C, 1.0 M $KNO_3$).

| N | Equilibrium | log β | | Δlog β |
|---|---|---|---|---|
| | | L-HisH | D-HisH | |
| 1 | $Cu^{2+} + GGY^{-} + HisH \rightleftharpoons Cu(GGY)(HisH)^{+}$ | 10.75 (1) | 10.76 (1) | −0.01 |
| 2 | $Cu^{2+} + GGY^{-} + His^{-} \rightleftharpoons Cu(GGY)(His)$ | 15.086 (3) | 14.983 (4) | **0.103** |
| 3 | $Cu^{2+} + GGY^{-} + His^{-} \rightleftharpoons Cu(GGY{\bullet}H_{-1})(His)^{-} + H^{+}$ | 6.72(1) | 6.74(2) | −0.02 |
| 4 | $Cu^{2+} + GGY{\cdot}H^{2-}_{-1} + His^{-} \rightleftharpoons Cu(GGY{\bullet}H_{-2})(His)^{2-} + H^{+}$ | 6.94(1) | 6.91(2) | 0.03 |
| 5 | $2Cu^{2+} + GGY^{-} + 2His^{-} \rightleftharpoons Cu_2(GGY{\bullet}H_{-1})(His)_2 + H^{+}$ | 20.65 (9) | 20.61 (8) | 0.04 |
| 6 | $2Cu^{2+} + GGY{\cdot}H^{2-}_{-1} + 2His^{-} \rightleftharpoons Cu_2(GGY{\bullet}H_{-3})(His)(HisH_{-1})^{3-} + 3H^{+}$ | 2.34(5) | 2.37(6) | −0.03 |

difference in formation constants with L- and D-histidine is bigger than double sum of standard deviations) is found only for the Cu(GGY)(His) form with the higher stability of complex with L-histidine.

The presence of stereoselectivity effects in the copper(II) – glycylglycyl-L-tyrosine – L/D-histidine system at 1:1:1 metal/ligand/ligand' ratio is also confirmed by spectrophotometric titration. Fig. 4 contains the dependencies of molar extinction coefficient on pH at several wavelengths. As can be seen from Fig. 4, the molar extinction coefficients at pH 6–8 are slightly different for systems with L- and D-histidine. The distribution diagram for system with L-histidine at spectrophotometric titration conditions is presented in Fig. 5 (electronic absorption spectra of the solutions are given in Fig. 10S).

The individual absorption spectra for mononuclear hetero-ligand complexes were obtained by mathematical modeling, taking into account the already obtained spectra of homo-ligand complexes for glycylglycyl-L-tyrosine (Fig. 2) and the spectra for histidine complexes from the previous investigation [1]. The results of such modeling are shown in Fig. 6 and spectral parameters of four mononuclear hetero-ligand complexes are summarized in Table 2S. Individual absorption spectra of hetero-ligand binuclear complexes were not obtained because of small accumulation fractions and many different complexes in solution.

As can be seen from the Fig. 6, the individual spectra of the form Cu (GGY)(His) are slightly different, whereas individual spectra of another

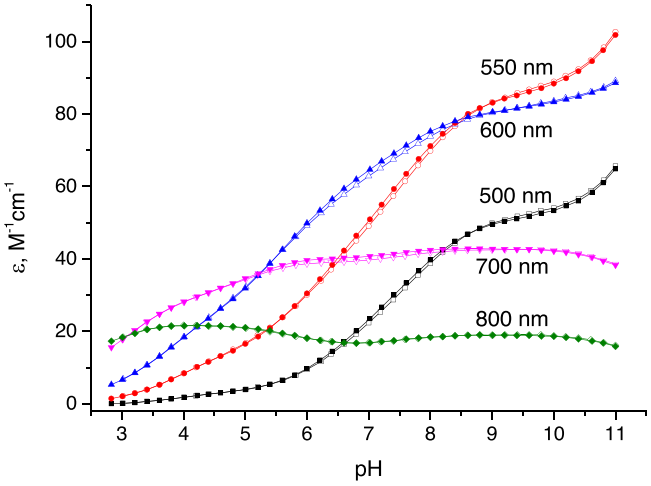


**Fig. 4.** Dependencies of molar extinction coefficient (ε) at different wavelengths on pH for the copper(II) – glycylglycyl-L-tyrosine – L/D-histidine system with the 1:1:1 metal/ligand/ligand' ratio at 25.0 °C; $c_{Cu(II)} = 9.850{\cdot}10^{-3}$ M, $c_{GGY{\cdot}H} = 1.004{\cdot}10^{-2}$ M, $c_{L\text{-}HisH} = 1.001{\cdot}10^{-2}$ M, $c_{GGY{\cdot}H} = 1.002{\cdot}10^{-2}$ M, $c_{D\text{-}HisH} = 1.001{\cdot}10^{-2}$ M; 1.0 M $KNO_3$. Open symbols corresponds to system with L-histidine, closed symbols – to D-histidine.

three heteroligand forms are very close for systems with L- and D-histidine. Those facts are in good agreement with the presence or absence of stereoselective effects by pH-potentiometry data.

Spectra of the forms $Cu(GGY{\bullet}H_{-1})(His)^{-}$ and $Cu(GGY{\bullet}H_{-2})(His)^{2-}$ with glycylglycyl-L-tyrosine are very similar and are close to the spectrum of the form $Cu(GGG{\bullet}H_{-1})(His)^{-}$ with glycylglycylglycine [5], which is evidence for the similar coordination of ligands in those forms.

The ternary system was also investigated by ESR spectroscopy. Examples of the ESR spectra are shown in Figs. 11S-13S, the parameters of the spectra are given in Table 4. It should be noted that in the area of accumulation of the Cu(GGY)(His) complex form, there are differences in the spectra of systems with different enantiomeric forms of histidine (Fig. 7), which confirms the stereoselectivity of the Cu(GGY)(His) formation. Some difference in spectral parameters is also observed for other heteroligand forms with glycylglycyl-L-tyrosine and L/D-histidine (see Table 4), however, due to the smaller accumulation of such forms, these

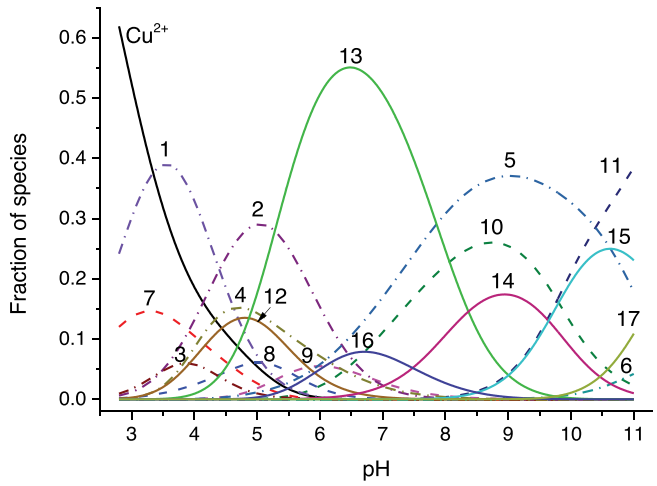


**Fig. 5.** Species distribution as a function of pH for the copper(II) – glycylglycyl-L-tyrosine – L-histidine system with the 1:1:1 metal/ligand/ligand' ratio at 25.0 °C; $c_{Cu(II)} = 9.850 \cdot 10^{-3}$ M, $c_{GGY \cdot H} = 1.004 \cdot 10^{-2}$ M, $c_{L\text{-}HisH} = 1.001 \cdot 10^{-2}$ M, 1.0 M $KNO_3$; 1 – $Cu(HisH)^{2+}$, 2 – $Cu(His)^{+}$, 3 – $Cu(HisH)_2^{2+}$, 4 – $Cu(His)(HisH)^{+}$, 5 – $Cu(His)_2$, 6 – $Cu(His)(HisH_{-1})^{-}$, 7 – $Cu(GGY\bullet H)^{2+}$, 8 – $Cu(GGY)^{+}$, 9 – $Cu(GGY\bullet H_{-1})$, 10 – $Cu(GGY\bullet H_{-2})^{-}$, 11 – $Cu(GGY\bullet H_{-3})^{2-}$, 12 – $Cu(GGY)(HisH)^{+}$, 13 – Cu(GGY)(His), 14 – $Cu(GGY\bullet H_{-1})(His)^{-}$, 15 – $Cu(GGY\bullet H_{-2})(His)^{2-}$, 16 – $Cu_2(GGY\bullet H_{-1})(His)_2$, 17 – $Cu_2(GGY\bullet H_{-3})(His)(HisH_{-1})^{3-}$.

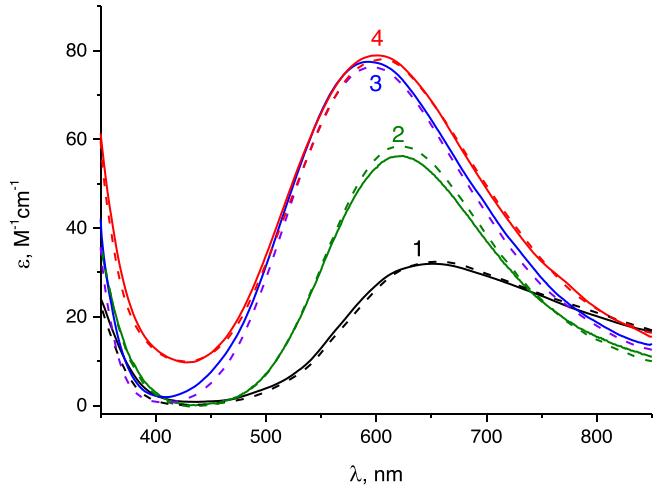


**Fig. 6.** Reconstructed electronic absorption spectra of the complexes in the copper(II) – glycylglycyl-L-tyrosine – L/D-histidine system at 25.0 °C on the 1.0 M $KNO_3$ background: 1 – $Cu(GGY)(HisH)^{+}$, 2 – Cu(GGY)(His), 3 – $Cu(GGY\bullet H_{-1})(His)^{-}$, 4 – $Cu(GGY\bullet H_{-2})(His)^{2-}$. Solid lines correspond to complexes with L-histidine, dashed lines – to D-histidine.

stereoselective effects cannot be considered as reliable.

Optimized structures of the Cu(GGY)(His) form with L- and D-isomers of amino acid are shown in Fig. 8. As can be seen from the Figure, the *cis*-arrangement of the amino groups of neighboring ligands is more favorable than the *trans*-arrangement both in the case of L- and D-histidine. This fact is evidence of a stronger *trans*-influence of the amino group compared to the carboxy-group and the imidazole fragment in the copper(II) coordination sphere. The most energetically favorable isomer of the Cu(GGY)(His) form is *cis*-isomer with L-histidine, which is in good agreement with the bigger formation constant of complex with L-histidine according to the experimental data (see Table 3). In the mentioned isomer the hydrogen bond between the phenoxyl group of tripeptide and the axially coordinated carboxy-group of amino acid is formed. Parallel orientation of the aromatic rings of neighboring ligands is evidence for π-π-stacking interaction, the distance between π-systems are near 3.5 Å,

**Table 4**
ESR spectra parameters of the heteroligand copper(II) complexes with glycyl-glycyl-L-tyrosine and L/D-histidine (r.t., 1.0 M $KNO_3$).

| N | Complex | $g_0$ | $A_0$, G | $A_N$, G |
|---|---|---|---|---|
| 1 | $Cu(GGY)(L\text{-}HisH)^{+}$ | 2.114(1) | 43(1) | not determined |
| 1′ | $Cu(GGY)(D\text{-}HisH)^{+}$ | 2.113(1) | 44(1) | not determined |
| 2 | Cu(GGY)(L-His) | 2.1190 (2) | 64.2 (4) | ~10 |
| 2′ | Cu(GGY)(D-His) | 2.1196 (2) | 62.9 (4) | ~10 |
| 3 | $Cu(GGY\cdot H_{-1})(L\text{-}His)^{-}$ | 2.102(1) | 66(1) | not determined |
| 3′ | $Cu(GGY\cdot H_{-1})(D\text{-}His)^{-}$ | 2.104(1) | 68(1) | not determined |
| 4 | $Cu(GGY\cdot H_{-2})(L\text{-}His)^{2-}$ | 2.111(1) | 71(1) | ~10 |
| 4′ | $Cu(GGY\cdot H_{-2})(D\text{-}His)^{2-}$ | 2.110(1) | 73(1) | ~10 |
| 5 | $Cu_2(GGY\cdot H_{-1})(L\text{-}His)_2$ | 2.106(3) | – | not determined |
| 5′ | $Cu_2(GGY\cdot H_{-1})(D\text{-}His)_2$ | 2.104(3) | – | not determined |
| 6 | $Cu_2(GGY\cdot H_{-3})(L\text{-}His)(L\text{-}HisH_{-1})^{3-}$ | 2.081(1) | – | not determined |
| 6′ | $Cu_2(GGY\cdot H_{-3})(D\text{-}His)(D\text{-}HisH_{-1})^{3-}$ | 2.082(1) | – | not determined |

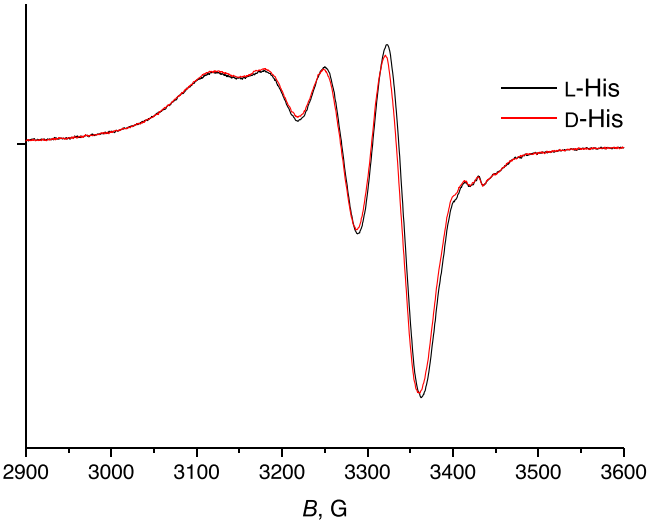


**Fig. 7.** Experimental EPR spectra of the copper(II) – glycylglycyl-L-tyrosine – L/D-histidine system at pH 6.60; $c_{Cu(II)} = 1.94 \cdot 10^{-2}$ M, $c_{GGY \cdot H} = 2.00 \cdot 10^{-2}$ M, $c_{HisH} = 2.00 \cdot 10^{-2}$ M; 1.0 M $KNO_3$, r.t.

which is typical for such interactions. In the *cis*-isomer with D-histidine the π-π-stacking interaction between the aromatic fragments is also present, but hydrogen bond in this case is formed between the phenoxyl group of tripeptide and the equatorially coordinated amino group of amino acid. Such hydrogen bonding does not seen to be favorable for the configuration of the tripeptide chain, resulting in less stability of the complex with D-histidine in comparison with L-histidine. In the *trans*-isomers of the Cu(GGY)(His) form the location of aromatic fragments is not suitable for π-π-stacking interaction (Fig. 8), which is an additional reason for big energy differences between *cis*- and *trans*-isomers of the Cu(GGY)(His) complex form.

Heteroligand binuclear complexes with tripeptides and amino acids deserve special attention. In the $Cu_2(GGY\bullet H_{-3})(His)(HisH_{-1})^{3-}$ form the deprotonated imidazole fragment acts as a bridge (Fig. 14S). This form is very similar with previously described heteroligand binuclear form with glycylglycylglycine [5], but the complex with tyrosine-containing tripeptide is more stable than complex with simplest tripeptide (see experimental data in Table 3 and data in work [5]), which can be explained by additional π-π-stacking interaction between imidazole bridge and tyrosine fragment of tripeptide and hydrogen bonding between the deprotonated phenoxyl group and amino group of histidine. In the case of glycylglycyl-L-tyrosine the axial coordination of imidazole bridge to the copper ion with coordinated tripeptide is more favourable

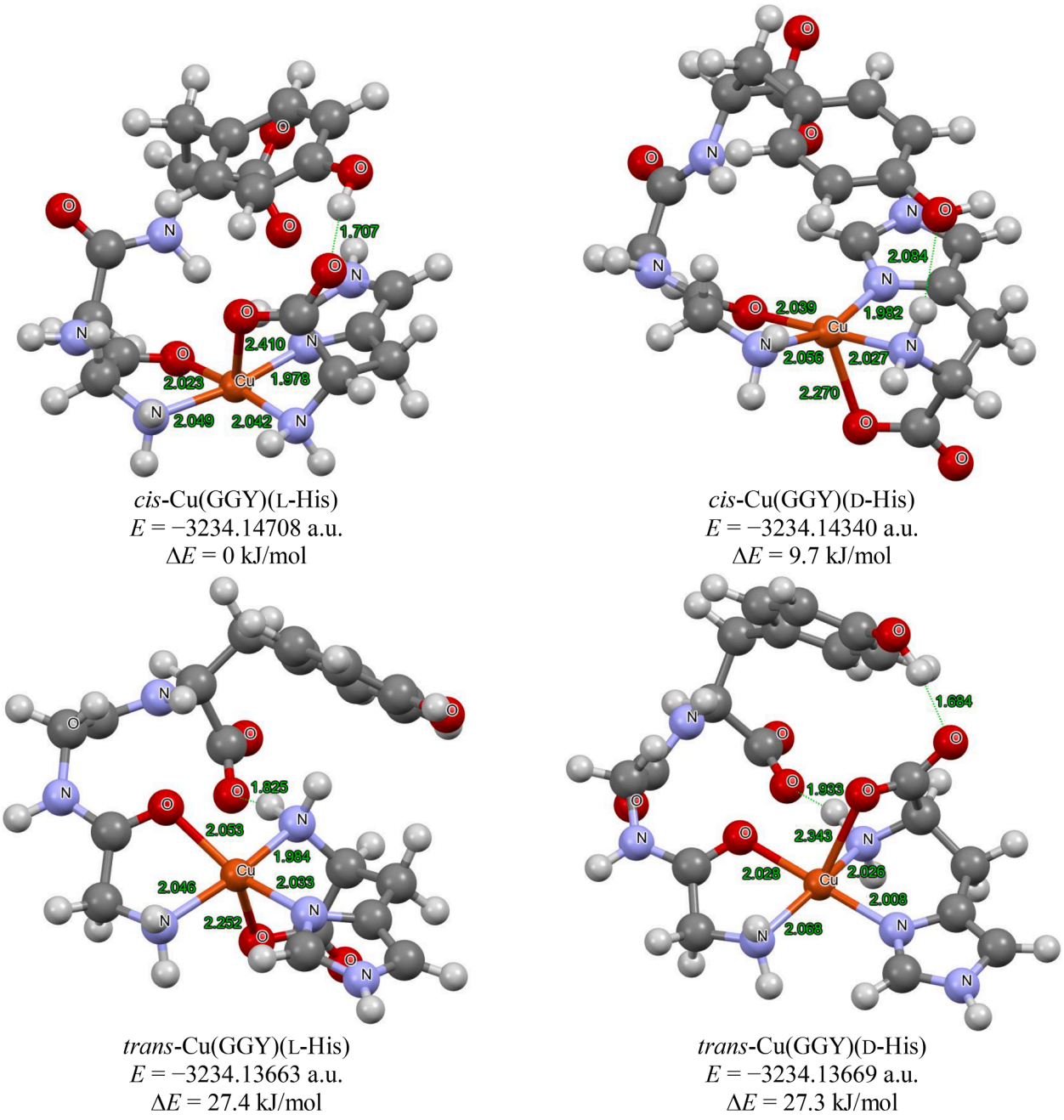


**Fig. 8.** Structures, formation energies (in atomic units, a.u.) and relative energies of the isomers of copper(II) complexes with glycylglycyl-L-tyrosine and L/D-histidine optimized on the B3LYP/TZVPP level with accounting solvent effects in the C-PCM model and dispersion correction (D3BJ).

than the equatorial one (see Fig. 14S) in contrast to the opposite situation in the case of glycylglycylglycine [5].

It should be mentioned that in the system with glycylglycyl-L-tyrosine one additional binuclear heteroligand form is presented – the $Cu_2(GGY{\bullet}H_{-1})(His)_2$ form, which is formed at neutral pH (see Fig. 5). This form is not presented in the system with glycylglycylglycine [5], because the imidazole bridge (which is not deprotonated in this case) needs additional stabilization by π-π-stacking interaction with tyrosine fragment (Fig. 14S). Such interaction is not possible in the case of glycylglycylglycine, that's why such form is less stable and is not detected in the copper(II) – glycylglycylglycine – histidine ternary system.

### 3.3. Substitution reaction kinetics in the copper(II) – glycylglycyl-L-tyrosine – L/D-histidine systems

In neutral and slightly alkaline medium (pH range from 7 to 9, see Fig. 1) the $Cu(GGY{\cdot}H_{-2})^{-}$ form is dominating. This complex form with two deprotonated peptide nitrogen atoms has an absorption maximum near 550 nm (see Fig. 2 and Table 1S) like the similar complex form with glycylglycylglycine [5]. Therefore, the tripeptide ligand for histidine substitution reaction kinetics was observed at this wavelength by stopped-flow method at pseudo-first order conditions (excess of histidine). Examples of kinetic dependencies at 1:1:15 metal/ligand/ligand' ratio are shown in Fig. 15S for the copper(II) – glycylglycyl-L-tyrosine – L-histidine system.

Final solutions spectra are the same with the spectrum of $Cu(His)_2$ form [1] which is evidence that the copper(II) *bis*-histidinate complex is

the final product of substitution reaction (situation is the same as in the case of glycylglycylglycine, see [5]). Additional confirmation for this conclusion is calculated on the base of thermodynamic data distribution diagram (Fig. 16S), where the mentioned form is dominating after reaching equilibrium at kinetic experiments conditions. Kinetic experiments results are shown in Figs. 9 and 17S for the systems with L- and D-histidine respectively in the form of the observed rate constant dependencies on pH. The reaction rate increases with increasing pH (situation is similar with previously described for glycylglycylglycine substitution by histidine [5]).

Glycylglycyl-L-tyrosine substitution by histidine can be described by three stages containing scheme which was proposed in previous work [5]. Hetero-ligand complex with tripeptide and histidine is formed at the first stage:

$$Cu(GGY{\cdot}H_{-2})^{-} + His^{-} \underset{k_{-1}}{\overset{k_1}{\leftrightarrow}} Cu(GGY{\cdot}H_{-2})(His)^{2-}$$

In the product of this stage the equatorially coordinated carboxy-group of glycylglycyl-L-tyrosine is replaced by amino group of histidine. Then the protonation and substitution of the peptide nitrogen atom between the second and third amino acid residues in the tripeptide takes place:

$$Cu(GGY{\cdot}H_{-2})(His)^{2-} + H_2O \underset{k_{-2}}{\overset{k_2}{\leftrightarrow}} Cu(GGY{\cdot}H_{-1})(His)^{-} + OH^{-}$$

The complete replacement of the glycylglycyl-L-tyrosine by the second molecule of histidine occurs at the last stage:

$$Cu(GGY{\cdot}H_{-1})(His)^{-} + His^{-} + H_2O \overset{k_3}{\rightarrow} Cu(His)_2 + GGY^{-} + OH^{-}$$

According to the experimental results the third stage is rate-determining and in the substitution process not only anionic, but also protonated form of histidine can be active:

$$Cu(GGY{\cdot}H_{-1})(His)^{-} + HisH \rightarrow Cu(His)_2 + GGY^{-}$$

It should be mentioned that unlike previously studied case with glycylglycylglycine, the kinetic dependencies for the system with glycylglycyl-L-tyrosine are adequately described only using two exponentials. The presence of the second faster exponent can be explained by the delayed entry of the first amino acid molecule due to the occupancy of all coordination positions in the initial complex with glycylglycyl-L-tyrosine (Fig. 3). Due to the insufficient number of points for a correct statistical estimate of the fast exponent, it is not considered in this paper.

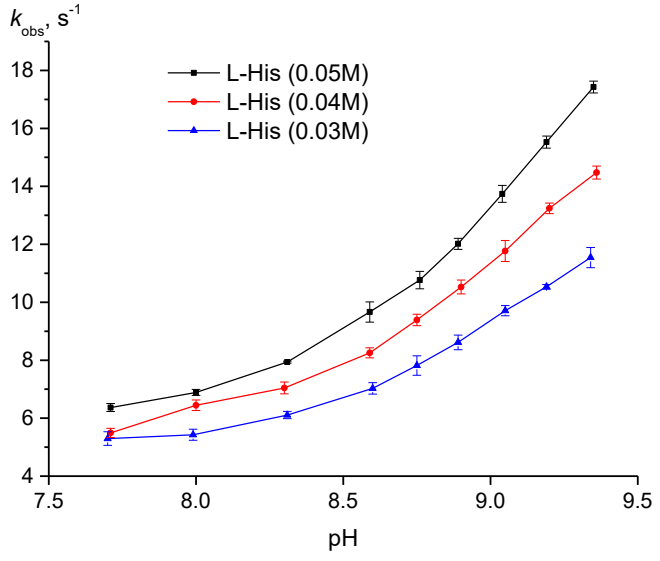


**Fig. 9.** Dependencies of the observed rate constant ($k_{obs}$) on pH at different histidine concentrations for the copper(II) – glycylglycyl-L-tyrosine – L-histidine (1:1:15) system at 25.0 °C obtained by stopped-flow method by mixing solutions I and II with registration at λ = 550 nm; I – Cu(II), GGY·H; II – L-HisH; $c_{tris}$ = 0.10 M, 1.0 M $KNO_3$.

At kinetic experiments conditions in solution only two mentioned forms of histidine are presented. On the base of this fact the observed rate constant can be represented by the following equation [5]:

$$k_{obs} = k_0 + k_L[His^-] + k_{LH}[HisH] = k_0 + k_{LH} \times c_{HisH} + (k_L - k_{LH})[His^-],$$

where $c_{HisH}$ is the total histidine concentration, $k_{obs}$ is the observed rate constant, $k_0$ is the substitution constant with the participation of the buffer, $k_L$ and $k_{LH}$ are the contributions from the anionic and protonated forms of the amino acid respectively. To determine all three contributions to the observed rate constant it is necessary to obtain the dependencies of the observed rate constant on the concentration of the anionic form of histidine at various overall amino acid concentrations. Such dependencies for glycylglycyl-L-tyrosine substitution by histidine are given in Figs. 10 and 18S for the systems with L- and D-histidine respectively. Calculated from the given dependencies kinetic results are presented in Table 5.

It should be mentioned that the substitution of glycylglycyl-L-tyrosine is slower than the substitution of glycylglycylglycine (compare Tables 5 in this paper and in the previous work [5]). This experimental fact can be explained by steric hindrance in the case of glycylglycyl-L-tyrosine, which has relatively big substituent in the third residue of tripeptide.

Statistically meaningful stereoselectivity is observed in the replacement of glycylglycyl-L-tyrosine by anionic form of histidine (see Table 5): the reaction rate is higher in the system with D-histidine. The manifestation of stereoselectivity in the substitution kinetics can be explained by the different structures of complexes with L- and D-histidine. It should be noted that the stereoselective effect for the Cu(GGY·H$_{-1}$)(His)$^-$ form, which is an intermediate in the substitution process, is not established in the thermodynamics of complex formation (see Table 3). The fact of the presence of significant stereoselectivity in the kinetics of substitution and its absence in the thermodynamics of complex formation is in good agreement with the associative mechanism of substitution, in which a *tris*-complex is formed (containing one tripeptide molecule and two histidine molecules), where the ligands are closer together than in *bis*-complex, thereby enhancing the stereoselective effect.

## 4. Conclusions

Complex formation in the copper(II) – glycylglycyl-L-tyrosine and copper(II) – glycylglycyl-L-tyrosine – L/D-histidine systems was investigated by pH-potentiometric titration and spectrophotometry methods in the pH range 2–11. Five homoligand and six heteroligand complexes were discovered for the first time. The structures of some complexes were optimized by DFT computations on the B3LYP/TZVPP level with the accounting solvent effect by the C-PCM model and dispersion correction (D3BJ). The individual absorption spectra and ESR spectra of some homoligand and heteroligand complexes were reconstructed.

The statistically meaningful stereoselective effect in the formation of Cu(GGY)(His) form with the higher stability of complex with L-histidine was revealed on the basis of pH-potentiometric titration data, confirmed by spectrophotometry, ESR spectroscopy and quantum-chemical calculations results and explained by the trans-influence and π-π-stacking interactions.

The kinetics of glycylglycyl-L-tyrosine substitution by L/D-histidine was investigated by stopped-flow technique with spectrophotometric detection and three-step scheme of the investigated process was used. Stereoselective effect in the tripeptide substitution by anionic form of

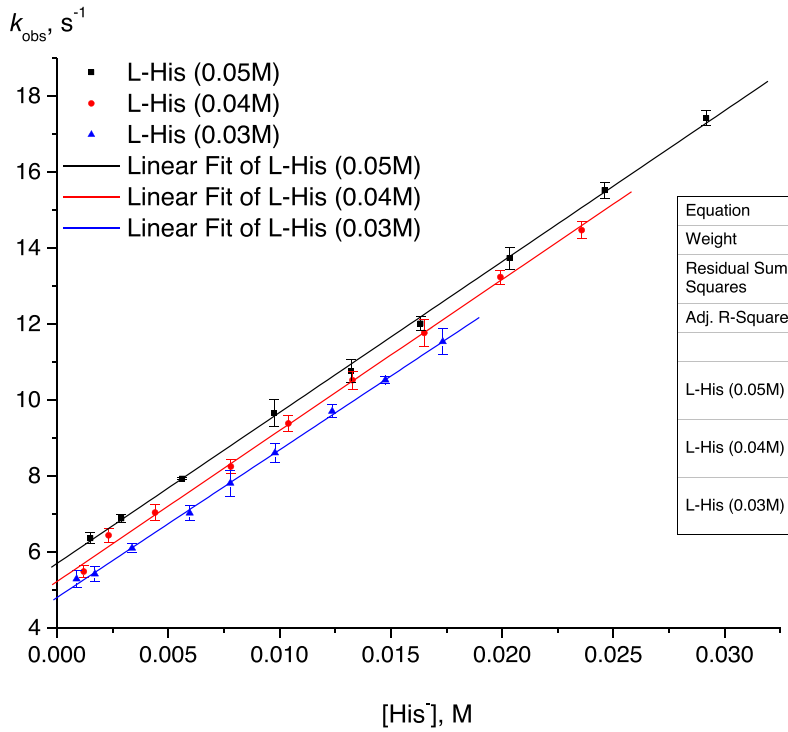


| Equation | y = a + b*x | | |
|---|---|---|---|
| Weight | Instrumental | | |
| Residual Sum of Squares | 2.1326 | 5.42734 | 1.0135 |
| Adj. R-Square | 0.99946 | 0.99698 | 0.99929 |
| | | Value | Standard Error |
| L-His (0.05M) | Intercept | 5.70496 | 0.02717 |
| | Slope | 397.26799 | 3.27522 |
| L-His (0.04M) | Intercept | 5.22915 | 0.09386 |
| | Slope | 397.43805 | 7.7355 |
| L-His (0.03M) | Intercept | 4.80776 | 0.04131 |
| | Slope | 388.50952 | 3.66516 |

**Fig. 10.** Dependencies of the observed rate constant ($k_{obs}$) on the concentration of the histidine anionic form [$His^-$] at different histidine concentrations for the copper(II) – glycylglycyl-L-tyrosine – L-histidine (1:1:15) system at 25.0 °C obtained by stopped-flow method by mixing solutions I and II with registration at λ = 550 nm; I – Cu(II), GGY·H; II – L-HisH; $c_{tris}$ = 0.10 M, 1.0 M $KNO_3$.

**Table 5**
Rate constants for the substitution reactions of glycylglycyl-L-tyrosine from the $Cu(GGY{\cdot}H_{-2})^-$ complex by L/D-histidine (25.0 °C, 0.1 M tris-buffer, 1.0 M $KNO_3$).

| Tripeptide | Amino acid | $k_0$, $s^{-1}$ | $k_{LH}$, $M^{-1}$ $s^{-1}$ | $k_L$, $M^{-1}$ $s^{-1}$ |
|---|---|---|---|---|
| glycylglycyl-L-tyrosine | L-histidine | 3.46 ± 0.03 | 44.9 ± 0.7 | 439 ± 5 |
| glycylglycyl-L-tyrosine | D-histidine | 3.37 ± 0.10 | 43.9 ± 3.1 | 459 ± 3 |

histidine with faster process for D-amino acid than for L-isomer of histidine was revealed and interpreted on the basis of the formation of heteroligand *tris*-complexes as intermediates in overall processes.

## Author contributions

All the authors made an equal contribution to the work.

## CRediT authorship contribution statement

**Nikita Yu. Serov:** Conceptualization, Methodology, Investigation, Writing – original draft, Writing – review & editing, Visualization, Formal analysis. **Valery G. Shtyrlin:** Conceptualization, Methodology, Investigation, Writing – review & editing, Visualization, Supervision, Formal analysis. **Mikhail S. Bukharov:** Investigation, Writing – review & editing, Formal analysis. **Anton V. Ermolaev:** Investigation, Formal analysis. **Edward M. Gilyazetdinov:** Investigation, Formal analysis. **Kira V. Urazaeva:** Investigation, Formal analysis. **Alexander A. Rodionov:** Investigation, Resources.

## Declaration of Competing Interest

The authors declare that they have no known competing financial interests or personal relationships that could have appeared to influence the work reported in this paper.

## Data availability

Data will be made available on request.

## Acknowledgements

The work was supported by Russian Foundation for Basic Research (RFBR) grant No 18-33-20072.

## Appendix A. Supplementary data

Supplementary data to this article can be found online at https://doi.org/10.1016/j.poly.2022.116176.

## References

[1] V.G. Shtyrlin, Y.I. Zyavkina, E.M. Gilyazetdinov, M.S. Bukharov, A.A. Krutikov, R. R. Garipov, A.S. Mukhtarov, A.V. Zakharov, Complex formation, chemical exchange, species structure, and stereoselective effects in the copper(II) - L/DL-histidine systems, Dalton Trans. 41 (2012) 1216–1228, https://doi.org/10.1039/c1dt11309g.
[2] V.G. Shtyrlin, E.M. Gilyazetdinov, N.Y. Serov, D.F. Pyreu, M.S. Bukharov, A. A. Krutikov, N.S. Aksenin, A.I. Gizatullin, A.V. Zakharov, Stability, lability, spectral parameters and structure of complexes and stereoselective effects in the nickel(II) – L/D/DL-histidine – L/D/DL-methionine systems, Inorg. Chim. Acta. 477 (2018) 135–147, https://doi.org/10.1016/j.ica.2018.02.018.
[3] B. Sarkar, Treatment of Wilson and Menkes diseases, Chem. Rev. 99 (1999) 2535–2544, https://doi.org/10.1021/cr980446m.
[4] R.H. Kretsinger, V.N. Uversky, E.A. Permyakov (Eds.), Encyclopedia of Metalloproteins, Springer New York, New York, NY, 2013.
[5] N.Y. Serov, V.G. Shtyrlin, M.S. Bukharov, A.V. Ermolaev, E.M. Gilyazetdinov, A. A. Rodionov, Complex structures, formation thermodynamics and substitution reaction kinetics in the copper(II) – glycylglycylglycine – L/D/DL-histidine system, Polyhedron 197 (2021), 115041, https://doi.org/10.1016/j.poly.2021.115041.
[6] H. Kozłowski, Spectroscopic and magnetic resonance studies on Ni(II), Cu(II) and Pd(II) complexes with Gly-Leu-Tyr and Tyr-Gly-Gly tripeptides, Inorg. Chim. Acta. 31 (1978) 135–140, https://doi.org/10.1016/s0020-1693(00)94990-9.

[7] T. Kiss, Copper(II) complexes of tyrosine-containing tripeptides, J. Chem. Soc., Dalton Trans. (1987) 1263, 10.1039/dt9870001263.
[8] B. Mrabet, M. Jouini, J. Huet, G. Lapluye, Potentiometric, calorimetric and spectroscopic study of copper(II) complexes of leucine-encephalin and tripeptides containing tyrosine, J. Chim. Phys. et Phys.-Chim. Biol. 89 (1992) 2187–2205.
[9] W.A. Franks, D. Van der Helm, The crystal and molecular structure of the dimeric copper(II) chelate of glycyl-L-leucyl-L-tyrosine, Acta Cryst. B 27 (1971) 1299–1310, https://doi.org/10.1107/s056774087100390x.
[10] D. Muller, B.-D.-L. Révérend, B. Sarkar, Studies of copper(II) binding to glycylglycyl-L-tyrosine-N-methyl amide, a peptide mimicking the $NH_2$-terminal copper(II)-binding site of dog serum albumin by analytical potentiometry, spectrophotometry, CD, and NMR spectroscopy, J. Inorg. Biochem. 21 (1984) 215–226, https://doi.org/10.1016/0162-0134(84)83005-6.
[11] P. Decock, B. Sarkar, Application of an advanced technique of data analysis by analytical potentiometry and comparison of results by SUPERQUAD. Studies of nickel(II) – glycine, copper(II) – glycylglycyl-L-tyrosine-N-methyl amide, and zinc (II) – 3,6-diazaoctane-1,8-diamine systems, Can. J. Chem. 65 (1987) 2804–2809, https://doi.org/10.1139/v87-466.
[12] A.A. Krutikov, V.G. Shtyrlin, A.O. Spiridonov, N.Y. Serov, A.N. Il'yin, M. S. Bukharov, E.M. Gilyazetdinov, New program for computation of the thermodynamic, spectral, and NMR relaxation parameters of coordination compounds in complex systems, J. Phys. Conf. Ser. 394 (2012), 012031, https://doi.org/10.1088/1742-6596/394/1/012031.
[13] S. Stoll, A. Schweiger, EasySpin, a comprehensive software package for spectral simulation and analysis in EPR, J. Magn. Reson. 178 (2006) 42–55, https://doi.org/10.1016/j.jmr.2005.08.013.
[14] F. Neese, The ORCA program system, WIREs Comput. Molec. Sci. 2 (2012) 73–78, https://doi.org/10.1002/wcms.81.
[15] W. Kohn, A.D. Becke, R.G. Parr, Density functional theory of electronic structure, J. Phys. Chem. 100 (1996) 12974–12980, https://doi.org/10.1021/jp960669l.
[16] A.D. Becke, Density-functional thermochemistry. III. The role of exact exchange, J. Chem. Phys. 98 (1993) 5648, 10.1063/1.464913.
[17] C. Lee, W. Yang, R.G. Parr, Development of the Colle-Salvetti correlation-energy formula into a functional of the electron density, Phys. Rev. B. 37 (1988) 785–789, https://doi.org/10.1103/PhysRevB.37.785.
[18] T. Yanai, D.P. Tew, N.C. Handy, A new hybrid exchange–correlation functional using the Coulomb-attenuating method (CAM-B3LYP), Chem. Phys. Lett. 393 (2004) 51–57, https://doi.org/10.1016/j.cplett.2004.06.011.
[19] A. Schäfer, C. Huber, R. Ahlrichs, Fully optimized contracted Gaussian basis sets of triple zeta valence quality for atoms Li to Kr, J. Chem. Phys. 100 (1994) 5829, https://doi.org/10.1063/1.467146.
[20] J.P. Perdew, K. Burke, M. Ernzerhof, Generalized gradient approximation made simple, Phys. Rev. Lett. 77 (1996) 3865–3868, https://doi.org/10.1103/PhysRevLett.77.3865.
[21] M. Cossi, N. Rega, G. Scalmani, V. Barone, Energies, structures, and electronic properties of molecules in solution with the C-PCM solvation model, J. Comput. Chem. 24 (2003) 669–681, https://doi.org/10.1002/jcc.10189.
[22] S. Grimme, J. Antony, S. Ehrlich, H. Krieg, A consistent and accurate ab initio parametrization of density functional dispersion correction (DFT-D) for the 94 elements H-Pu, J. Chem. Phys. 132 (2010), 154104, https://doi.org/10.1063/1.3382344.
[23] S. Grimme, S. Ehrlich, L. Goerigk, Effect of the damping function in dispersion corrected density functional theory, J. Comput. Chem. 32 (2011) 1456–1465, https://doi.org/10.1002/jcc.21759.